Neuropharmacology. Author manuscript; available in PMC 2016 August 01.

Published in final edited form as:
Neuropharmacology. 2015 August ; 95: 377–387. doi:10.1016/j.neuropharm.2015.04.015.

Carbonic anhydrase inhibition by acetazolamide reduces *in vitro* epileptiform synchronization

Shabnam Hamidi and **Massimo Avoli***
Montreal Neurological Institute, Department of Neurology & Neurosurgery, McGill University, 3801 University Street, Montréal, QC, H3A 2B4, Canada

Abstract

Depolarizing $GABA_A$ receptor-mediated currents are contributed by HCO_3^- efflux, and play a role in initiating ictal-like epileptiform events in several cortical structures supporting the view that $GABA_A$ receptor signaling actively participates to epileptiform synchronization. We employed here field potential recordings to analyze the effects of the carbonic anhydrase inhibitor acetazolamide (10 μM) on the epileptiform activity generated *in vitro* by piriform and entorhinal cortices (PC and EC, respectively) during application of the K^+ channel blocker 4-aminopyridine (4AP, 50 μM). Under these experimental conditions ictal- and interictal-like discharges along with high-frequency oscillations (ripples: 80–200 Hz, fast ripples: 250–500 Hz) occurred in these two regions. In both PC and EC, acetazolamide: (i) reduced the duration and the interval of occurrence of ictal discharges along with the associated ripples and fast ripples; (ii) decreased the interval of occurrence of interictal discharges and the rates of associated fast ripples; and (iii) diminished the duration and amplitude of pharmacologically isolated GABAergic events while increasing their interval of occurrence. Our results indicate that acetazolamide effectively controls 4AP-induced epileptiform synchronization in PC and EC. We propose that this action may rest on decreased $GABA_A$ receptor-mediated efflux leading to diminished depolarization of principal cells and, perhaps, of interneurons.

Keywords

4-Aminopyridine; Carbonic anhydrase; Entorhinal cortex; Epilepsy; GABA; High-frequency oscillations; Piriform cortex

1. Introduction

The role of $GABA_A$ receptor-mediated signaling in epilepsy has been questioned for a long time. Early work in the *in vitro* hippocampal slice preparation demonstrated that interictal epileptiform activity results from weakened inhibition (Schwartzkroin and Prince, 1978, 1980; Johnston and Brown, 1981) but later, prolonged epileptiform discharges were identified during experimental procedures that enhance GABAergic signaling such as the K^+

*Corresponding author. Tel.: +1 514 998 6790; fax: +1 514 398 8106. massimo.avoli@mcgill.ca (M. Avoli).

Conflicts of interest
None of the authors has any conflict of interest to disclose.

channel blocker 4-aminopyridine (4AP) or Mg^{2+} free medium (Avoli, 1990; see for review Avoli and de Curtis, 2011), thus underscoring different and possibly conflicting roles of $GABA_A$ receptor-mediated inhibition in epileptiform synchronization.

$GABA_A$ receptor activation opens channels that are permeable to Cl^- and to a lesser extent to HCO_3^-. In adulthood the $GABA_A$ receptor-mediated current is hyperpolarizing thanks to the activity of a cation chloride cotransporter that maintains intracellular [Cl^-] low (Farrant and Kaila, 2007; Blaesse et al., 2009). Another prerequisite for hyperpolarization is that at resting membrane potential the $GABA_A$ receptor-mediated HCO_3^- inward current is not larger than the Cl^- outward current (Kaila, 1994; Rivera et al., 2005). Although, GABA principally induces hyperpolarizing inhibition in postsynaptic neurons, it can also exert depolarizations (Andersen et al., 1980; Alger and Nicoll, 1982). Relevant to the field of epilepsy research, $GABA_A$ receptor-mediated signaling has been shown to be involved in the initiation and maintenance of ictal discharges (see for review Avoli and de Curtis, 2011). Moreover, several studies have suggested that “depolarizing GABA” is contributed by HCO_3^- efflux (Grover et al., 1993; Perez Velazquez, 2003; Ruusuvuori et al., 2004). Specifically, prolonged activation of $GABA_A$ receptors should lead to an excessive load of Cl^- into the postsynaptic neuron resulting in degradation of the Cl^- driving force (Staley et al., 1995). Under these conditions, HCO_3^- current would become dominant thus depolarizing the postsynaptic neuron since the intracellular HCO_3^- is consistently replenished by the carbonic anhydrase activity (Kaila et al., 1997; Voipio and Kaila, 2000).

Networks of inhibitory GABAergic interneurons can promote synchronicity in many brain structures due to their high connectivity ratio (Jefferys et al., 2012a). This synchronous GABAergic signaling has also been proposed to play a role in the generation of high frequency oscillations (HFOs) that are recorded in the EEG of epileptic patients and in animal models of temporal lobe epilepsy (see for review Jefferys et al., 2012b). HFOs can also be recorded *in vitro* in brain structures such as the piriform cortex (PC) and the entorhinal cortex (EC) (Avoli et al., 2013; Hamidi et al., 2014; Herrington et al., 2014) during application of 4AP that is known to enhance both excitatory and inhibitory transmitter release.

To date the role played by the $GABA_A$ receptor-mediated HCO_3^- efflux in epileptiform synchronization and in particular its participation to ictogenesis remains unclear. Therefore, in this study we investigated the effects induced by the carbonic anhydrase inhibitor acetazolamide on the epileptiform discharges and associated HFO that are generated by rat olfactory (PC) and limbic (EC) cortical networks maintained *in vitro* during 4AP treatment.

2. Methods

2.1. Brain slice preparation and maintenance

Male, adult Sprague-Dawley rats (250–275 g) were decapitated under isoflurane anesthesia according to the procedures established by the Canadian Council of Animal Care. The brain was quickly removed and placed in cold (1–3 °C), oxygenated artificial cerebrospinal fluid (ACSF) with the following composition (mM): 124 NaCl, 2 KCl, 2 $CaCl_2$, 2 $MgSO_4$, 1.25

KH_2PO_4, 26 $NaHCO_3$, 10 D-glucose. Horizontal brain slices (450 μm) containing PC and EC were cut from this brain block using a vibratome. Slices were then transferred to an interface tissue chamber where they were superfused with ACSF and humidified gas (95% O_2, 5% CO_2) at a temperature of 31–32 °C and a pH of 7.4. In nominally CO_2/HCO_3^--free N-2-hydroxyethylpiperazine-N′-2-ethanesulfonic acid (HEPES)-buffered medium, NaHCO3 was replaced by 20 mM HEPES, and the solution was gassed with 100% O_2; in these experiments the pH was adjusted to 7.4 with NaOH. 4AP (50 μM), acetazolamide (ACTZ, 10 μM), benzolamide (BA, 10 μM), 3, 3-(2-carboxypiperazin-4-yl)-propyl-1-phosphonate (CPP, 10 μM), 6-cyano-7-nitroquinoxaline-2, 3-dione (CNQX, 10 μM) and picrotoxin (PTX, 100 μM) were bath applied. Chemicals were acquired from Sigma–Aldrich Canada (Oakville, Ontario, Canada) except for BA that was generously provided by Dr. Kai Kaila at the University of Helsinki (Helsinki, Finland).

2.2. Electrophysiological recordings

Field potential recordings, which were sampled at 5000 Hz were obtained 50 min after the application of 4AP with ACSF-filled, glass pipettes (1B150F-4;World Precision Instruments, Sarasota, Florida, USA; tip diameter <10 μm, resistance 5–10 MΩ) that were connected to high-impedance amplifiers. After 25–40 min recordings in the presence of 4AP, any given drug was applied and recordings were continued for 60–90 min. The recording electrodes were positioned in the deep layers of the posterior PC and of the lateral EC. Field potential signals were fed to a computer interface (Digidata 1322A, Molecular Devices, and Palo Alto, CA, USA), acquired and stored using the PCLAMP 9.2 software (Molecular Devices). Subsequent data analyses were performed with CLAMPFIT 9.2 (Molecular Devices).

2.3. Detection of high-frequency oscillatory events

Time-periods containing ictal and interictal discharges recorded from the PC and EC were extracted. To identify oscillations in each frequency range (80–200 Hz and 250–500 Hz), a multi-parametric algorithm was employed using routines based on standardized functions (Matlab Signal Processing Toolbox) as described in detail in Salami et al. (2012) and Hamidi et al. (2014).

To be considered as HFOs, oscillatory events in each frequency range had to show at least four consecutive cycles, having amplitude of 3 SD above the mean of the reference period. The time lag between two consecutive cycles had to be between 5 and 12.5 ms for ripples (80–200 Hz) and between 2 and 4ms for fast ripples (250–500 Hz). Oscillatory events containing overlapping ripples and fast ripples were excluded from the analysis (Bénar et al., 2010).

2.4. Statistical analysis

We used CLAMPFIT 9.2 (Molecular Devices) for offline analysis of the duration and interval of occurrence of ictal and interictal discharges. To segregate ictal from interictal discharges, we applied the k-means clustering algorithm with squared euclidean distances on the duration of all recorded events. Appropriate clustering of data was obtained with two groups, with a cutoff at 3 s. Therefore, all events ≥3 s were considered as ictal activity, whereas those lasting <3 s were considered as interictal events (The distribution of the event

duration is summarized in Fig. 2A). These values are similar to those “arbitrarily” chosen by Traub et al. (1996). The same cutoff at 3 s was also used to segregate ictal and interictal discharges after application of ACTZ. The duration of both ictal and interictal discharges were defined as the time between the first deflection of the discharge from baseline to its return to baseline. The interval of occurrence of both ictal and interictal discharges were defined as the time between the onsets of two consecutive discharges. Amplitude of epileptiform events was measured from peak to peak. Since the kurtosis and skewness measures showed that values were not normally distributed, we transformed the raw data to Z-scores and performed One-way ANOVAs followed by Tukey post-hoc tests to identify differences between experimental conditions (i.e., 4AP alone, and 4AP+ ACTZ) in each region (PC and EC) regarding the rate and duration of ictal events and the rate, duration and amplitude of interictal discharges and isolated GABAergic events.

When analyzing the dynamics of HFO occurrence, in order to account for differences in duration, ictal discharges were transformed into a time scale from 0 (start of the ictal event) to 100 (end of the ictal event). The ictal period was then divided in three parts and rates of ripples and fast ripples in each region (PC and EC) were compared using non-parametric Wilcoxon signed rank tests followed by Bonferroni–Holm corrections for multiple comparisons. This allowed us to evaluate if ripples or fast ripples predominated at specific moments of the ictal event in different experimental conditions (i.e., 4AP alone, and 4AP+ ACTZ) in each region. Statistical tests were performed in Matlab R2012b (Matworks, Natick, MA) and the level of significance was set at $p < 0.05$. Results are expressed as Mean ± SEM and *n* indicates the number of slices used for analysis.

3. Results

3.1. Effects of carbonic anhydrase inhibition on 4AP-induced epileptiform activity

Field potential recordings – which were obtained simultaneously from PC and EC during 4AP application – revealed ictal and interictal discharges that occurred in both structures (Hamidi et al., 2014) (Fig. 1). Ictal discharges recorded from PC lasted 98.67 ± 12.02 s, and recurred every 169.01 ± 10.41 s (69 events, n = 10 experiments) whereas those occurring in EC lasted 132.31 ± 13.17 s, and recurred every 184.16 ± 10.58 s (60 events, n = 10 experiments). Interictal discharges recorded from PC (45 events, n = 10 experiments) and EC (50 events, n = 10 experiments) in these experiments lasted 1.88 ± 0.34 s and 2.01 ± 0.21 s, occurred every 57.5 ± 3.7 s and 49.9 ± 5.8 s, and had amplitudes of 1.28 ± 0.09 mV and 1.38 ± 0.18 mV, respectively.

As illustrated in Fig. 1, 20 min application of ACTZ (10 μM) disrupted the pattern of epileptiform discharge recorded from PC and EC under control conditions. Specifically, ACTZ (10 μM) abolished the prolonged ictal discharges seen under control conditions and disclosed a continuous pattern of synchronous epileptiform events lasting between 2 and 16 s. As illustrated in Fig. 2A ACTZ (10 μM) caused a significant change in the distribution of epileptiform discharge duration ($p < 0.0001$) in both areas. Using cutoff point between ictal and interictal discharges at 3 s, we were able to analyze the interval of occurrence of these events. In both PC and EC, ACTZ (10 μM) induced a significant decrease ($p < 0.0001$) in the interval of occurrence of ictal discharges to 53.9 ± 7.7 s and 82.5 ± 8.7 s, respectively (Fig.

2B, n = 10 experiments). To determine whether net effect of acetazolamide on epileptiform discharges is anticonvulsive, we compared the cumulative duration of epileptiform activity in time windows of 30 min before and during ACTZ (10 μM) application. Application of ACTZ (10 μM) reduced the cumulative duration of ictal discharges from 465.2 ± 41.6 s to 201.1 ± 46.8 s in PC and from 428.3 ± 80.7 s to 143.4 ± 22.1 s in EC (Fig. 2B, n = 10 experiments, $p < 0.01$). We also analyzed the effect of ACTZ (10 μM) on the interval of interictal discharges recorded from PC and EC. As illustrated in Fig. 2C, we found that application of ACTZ (10 μM) resulted in a reduction in the interval of occurrence of interictal discharges to 34.9 ± 3.2 s in PC and to 38.7 ± 2.7 s in the EC (Fig. 2C, n = 10 experiments, $p < 0.01$).

The role of carbonic anhydrase in the generation of the long-lasting ictal discharges was further confirmed by recordings performed in HCO_3^--free HEPES-buffered solution. Withdrawal of CO_2/HCO_3^- for 20 min completely blocked the ictal discharges in both PC and EC (Fig. 3A, *n* = 6 experiments). These results suggest that ACTZ (10 μM) effects are not presumably due to acidification (a process that may affect neurotransmitter release and gap junction function) but rather to its ability to block intracellular carbonic anhydrase. Next, we used BA (10 μM), an impermeable carbonic anhydrase inhibitor that only blocks extracellular carbonic anhydrase (Fig. 3B, *n* = 4 experiments). As shown in Fig. 3C, after 60 min of application of BA (10 μM), ictal discharges continued to occur with the same frequency whereas HCO_3^--free HEPES-buffered solution completely blocked occurrence of ictal discharges after 20 min in both PC and EC. As it shown in Fig. 4, HCO_3^--free HEPES-buffered solution disrupted the pattern of epileptiform discharge recorded from PC and EC under control conditions in a way that it abolished the prolonged ictal discharges seen under control conditions and reduced the duration of interictal discharges significantly ($p < 0.001$) from 1.32 ± 0.06 s to 0.83 ± 0.04 s in PC and from 2.11 ± 0.05 to 1.14 ± 0.09 s in EC. On the other hand, in the presence of BA both interictal and long-lasting ictal discharges continued to occur and application of BA did not affect the distribution of duration of these epileptiform events significantly (Fig. 4).

Next, to confirm that the effects induced on the epileptiform activity by either carbonic anhydrase inhibition or HCO_3^--free HEPES-buffered solution was due the contribution of HCO_3^- efflux via $GABA_A$ receptor-mediated mechanism, we used the $GABA_A$ receptor antagonist PTX (100 μM). PTX abolished the long-lasting ictal events within 10 min of application and disclosed epileptiform discharges lasting 1–6 s in both PC and EC (Fig. 5A, n = 6 experiments). Further application of ACTZ (10 μM) did not change the duration (Fig. 5B) and interval of occurrence (Fig. 5C) of these epileptiform discharges.

3.2. Effects of ACTZ on high frequency oscillation

We also analyzed the occurrence of ripples (80–200 Hz) and fast ripples that were associated to ictal and interictal discharges recorded from the PC and EC under control conditions (i.e., 4AP application) and in the presence of 10 μM ACTZ (Fig. 6A and B, n = 10 experiments). Application of ACTZ (10 μM) reduced the cumulative number of ripples per ictal discharge from 32.13 ± 7.99 to 16.22 ± 6.42 in PC and from 39.00 ± 6.52 to 22.65 ± 6.13 in EC (Fig. 6C, $p < 0.05$). Application of ACTZ (10 μM) also led to a reduction of the cumulative

number of fast ripples per ictal from 94.88 ± 21.35 to 58.50 ± 9.75 in PC and from 91.80 ± 23.46 to 52.38 ± 17.50 in EC (Fig. 6C, $p < 0.05$).

To rule out the possibility that the reduction in the average number of ripples and fast ripples during ACTZ application was caused by the decrease in duration of ictal discharges, we normalized the duration of ictal discharges by transforming them into a time scale from 0 (start of the ictal event) to 100 (end of the ictal event). In the PC, application of 10 μMACTZ led to a significant decrease of ripples and fat ripples occurrence throughout the duration of ictal discharges ($p < 0.001$) (Fig. 7A, PC). Also in the EC, the rate of occurrence of ripples and fast ripples were significantly ($p < 0.001$) decreased following the application of 10 μM ACTZ (Fig. 7A, EC).

Ripples and fast ripples also occurred in coincidence with interictal discharges. Under 4AP alone, only 2% (1/45) of interictal spikes recorded in the PC co-occurred with ripples, whereas 11.1% of them (5/45) co-occurred with fast ripples (Fig. 7B, PC, n = 10 experiments). In the EC, HFO occurrence was higher than in PC with 4% of interictal discharges (2/50) co-occurring with ripples and 22% of them (11/50) co-occurring with fast ripples (Fig. 7B, EC). In the PC, application of 10 μM ACTZ did not change the occurrence of ripples associated with interictal spikes (3/171 events) while it induced a significant ($p < 0.05$) decrease in the occurrence of fast ripples associated with interictal spikes to 4% (7/171 events, n = 10 experiments). In the EC as well, while ripple occurrence did not change significantly (3/137 events) application of ACTZ (10 μM) led to a significant ($p < 0.05$) decrease in the occurrence of fast ripples associated with interictal spikes to 10.9% (15/137 events, Fig. 7B, n = 10 experiments). Thus, ACTZ (10 μM) can significantly reduce the proportion of fast ripples associated to interictal discharges recorded from both PC and EC.

3.3. Effects of acetazolamide on pharmacologically isolated synchronous events

Finally, we blocked glutamatergic ionotropic transmission with CPP and CNQX (10 μM each) to analyze the effects of ACTZ (10 μM) on the 4AP-induced pharmacologically isolated GABAergic events (see for review Avoli and de Curtis, 2011; Hamidi et al., 2014). Blocking carbonic anhydrase activity with ACTZ (10 μM) induced a reduction in the duration of these GABAergic synchronous potentials from 3.47 ± 0.12 s to 2.62 ± 0.09 s in PC and from 2.43 ± 0.3 s to 1.48 ± 0.17 s in EC (Fig. 8C, n = 6 experiments, $p < 0.05$). Moreover, application of 10 μM ACTZ increased significantly ($p < 0.001$) the interval of occurrence of the pharmacologically isolated events from 59.65 ± 3.13 s to 92.19 ± 3.26 s in PC but not in the EC (Fig. 8C). Finally in both PC and EC, ACTZ (10 μM) decreased significantly the amplitude of these synchronous events from 1.15 ± 0.08 mV to 0.37 ± 0.01 mV and from 0.62 ± 0.04 mV to 0.29 ± 0.02 mV, respectively (Fig. 8C, $p < 0.0001$).

4. Discussion

The new findings of our study can be summarized as follows. First, blocking carbonic anhydrase activity with ACTZ or using HCO_3^--free HEPES-buffered solution disrupted the pattern of epileptiform activity and markedly reduced the duration of the ictal discharges in both PC and EC. Second, ACTZ decreased the interval of occurrence of 4AP-induced ictal and interictal discharges in both PC and EC. Third, ACTZ decreased the occurrence of

ripples and fast ripples throughout the duration of ictal discharges in both regions. Fourth, this pharmacological procedure led to a reduction in the occurrence of fast ripples associated to interictal discharges in both regions. Finally, blocking carbonic anhydrase activity led to a decrease in the duration and amplitude and to an increase (in the PC, only) in the interval of occurrence of pharmacologically isolated synchronous GABAergic events.

4.1. Blocking carbonic anhydrase activity reduces 4AP-induced epileptiform events

We have found that blocking carbonic anhydrase activity by application of ACTZ (Stinger, 2000; Supuran et al., 2003) disrupted the pattern of occurrence of epileptiform discharges in both PC and EC, and made the typical ictal discharges induced by 4AP – which are characterized by tonic and clonic phases – disappear. Furthermore, this pharmacological procedure reduced the interval of occurrence of ictal and interictal discharges. $GABA_A$ receptor-mediated signaling is associated to outward Cl^- and inward HCO_3^- currents (Krnjević, 1974; Grover et al., 1993; Farrant and Kaila, 2007), and it has been demonstrated that carbonic anhydrase activity replenishes HCO_3^- intracellularly (Kaila et al., 1997; Voipio and Kaila, 2000). Although, Cl^- and HCO_3^- currents flow in opposite directions, they do not cancel out each other since Cl^- permeates through the GABA channels more rapidly than HCO_3^- (Staley, 2004). Therefore, $GABA_A$ receptor mediated signaling is normally hyperpolarizing, and thus inhibitory, due to the low intracellular [Cl^-] in postsynaptic cells. However, in some circumstances such as repetitive activation of $GABA_A$ receptors, GABAergic transmission can become depolarizing (Farrant and Kaila, 2007).

The inward HCO_3^- current can contribute to the $GABA_A$ receptor-mediated depolarizations since it has a quite positive reversal potential (i.e.,−10 to −15 mV) (Staley et al., 1995; Rivera et al., 2005). In addition, prolonged activation of $GABA_A$ receptor leads to accumulation of Cl^- inside the postsynaptic cell that can overwhelm the K^+-Cl^- cotransporter (KCC2) activity and eventually, results in the depolarizing $GABA_A$ mediated signaling through degradation of Cl^- current and dominance of HCO_3^- current (Staley, 2004). This HCO_3^- dependent GABA-mediated depolarizing may results in activation of voltage-gated Ca^{2+} channels and uptake of Ca^{2+} in the postsynaptic cells; both events are indeed blocked by application of carbonic anhydrase inhibitors or by using HCO_3^--free HEPES-buffered solution (Autere et al., 1999). Interestingly, and in support of the contribution of HCO_3^- currents to epileptiform synchronization the antiepileptic drug topiramate exerts its effect by inhibiting carbonic anhydrase activity (Dodgson et al., 2000). The results observed during application of ACTZ is presumably not due to the small amount of acidification induced by blockade of carbonic anhydrase (Ruusuvuori et al., 2013) since using HCO_3^--free HEPES-buffered solution also had the same effect and it completely blocked the occurrence of ictal discharges in both PC and EC. The small changes in intracellular pH can trigger the activation of Na^+-coupled anion exchanger (NDAE) (Schwiening and Boron,1994), which extrudes Cl^- and H^+ and loads HCO_3^- and Na^+ (Payne et al., 2003; Hubner and Holthoff, 2013) and might result in replacement of HCO_3^- inside the cell. This might explain why bath applying HCO_3^--free HEPES-buffered solution leads to a complete blockade of ictal discharges in both PC and EC whereas application of ACTZ only abolished the long-lasting ictal events. In addition, activation of NDAE can result in the

extrusion of Cl^- that can promote the inhibitory action of GABA by maintaining Cl^- reversal potential negative to the resting membrane potential (Hübner and Holthoff, 2013). Another anion exchanger, AE3, which is responsible for extrusion of HCO_3^- and load of Cl^-, is probably inactive because of the high intracellular [Cl^-] (due to the prolonged activation of $GABA_A$ receptor) and low intracellular [HCO_3^-] (due to the blockade of carbonic anhydrase activity).

4.2. Carbonic anhydrase blocker can modulate interictal and ictal HFOs

We have found that ictal events recorded from PC and EC contain less ripples and fast ripples during application of ACTZ as well as that these effects were accompanied by reduced occurrence of fast ripples associated with interictal discharges in both PC and EC. It has been proposed that ripples reflect IPSPs generated by principal neurons entrained by a network of synchronously active interneurons (Buzsaki et al., 1992; Ylinen et al., 1995), while fast ripples would not strictly depend on GABA receptor signaling (Dzhala and Staley, 2003; Engel et al., 2009; Bragin et al., 2011). In fact, it is believed that fast ripples may be generated primarily by the synchronous activity of principal neurons since blockade of ionotropic glutamatergic signaling attenuates fast ripples (Jefferys et al., 2012b). Blocking production of HCO_3^- by inhibiting carbonic anhydrase activity affects $GABA_A$ receptor-mediated signaling and in consequence, generation of ripples and fast ripples associated with ictal and interictal discharges. These changes could reflect a decrease in the excitability in both principal neurons and interneurons. The ACTZ-induced depression in excitability leading to a decrease in the epileptiform synchronization along with HFOs further supporting the idea that HFOs can be a marker of epileptiform excitability (Jefferys et al., 2012b; Lévesque et al., 2012).

4.3. Modulation of isolated GABAergic events by carbonic anhydrase blocker

We have confirmed here that ionotropic glutamatergic receptor-mediated signaling is required for the generation of ictal discharges in both PC and EC (Avoli et al., 2013; Hamidi et al., 2014; Herrington et al., 2014). In keeping with evidence obtained in these previous studies, we have found that blockade of glutamatergic signaling using NMDA and non-NMDA receptor antagonists led to the occurrence of isolated, slow GABA receptor-dependent potentials during application of 4AP. These glutamatergic independent field potentials result from the synchronous firing of interneurons that leads to GABA release and consequent postsynaptic activation of principal cells (Avoli and de Curtis, 2011).

We have found here that blocking carbonic anhydrase activity shortened the duration of these synchronous events, and reduced their amplitude in both PC and EC; in addition, this pharmacological procedure led to a decrease in the rate of occurrence of these events in PC. These findings, therefore, demonstrate for the first time that $GABA_A$ receptor-dependent $HCO3^-$ efflux, which is reduced and perhaps blocked by ACTZ, contributes the generation of the synchronous GABAergic events induced by 4AP. Indeed, these field events are blocked by $GABA_A$ receptor antagonists and correspond to transient depolarizations of principal cells in several limbic structures (see for review Avoli and de Curtis, 2011). In addition, application of $GABA_A$ receptor antagonist, PTX, had effects similar to those induced by ACTZ on 4AP-induced epileptiform discharges and further application of ACTZ

did not change the duration and interval of occurrence of these epileptiform events. These findings further confirm the contribution of $GABA_A$ receptor-dependent HCO_3^- efflux in the maintenance of epileptiform events. However, one should not overlook the contribution given to these synchronous GABAergic events by the Cl^- dependent increases in the extracellular $[K^+]$ that are presumably caused by KCC2 activity (Kaila et al., 1997; Viitanen et al., 2010).

5. Conclusions

Our results show that during application of 4AP, blocking carbonic anhydrase activity by ACTZ decreases epileptiform synchronization by abolishing the long-lasting tonic-clonic ictal discharges in both PC and EC. A similar effect has recently been identified in organotypic slice culture preparation by Lillis et al. (2012). We have also found that blocking carbonic anhydrase activity reduces the occurrence of HFOs associated with epileptiform discharges in both regions. Our findings support the view that $GABA_A$ receptor-mediated signaling actively participates in generation and maintenance of epileptiform synchronization as suggested in several experimental models as well as by the fact that blocking $GABA_A$ receptor with $GABA_A$ receptor antagonists abolishes the occurrence of ictal discharges. In conclusion, our findings substantiate further the role of GABA signaling and interneuronal networks in driving neuronal populations toward hypersynchronous states (Avoli and de Curtis, 2011; Miles et al., 2012).

Acknowledgments

This study was supported by the Canadian Institutes of Health Research (CIHR grants 8109 and 74609). We thank Dr. M. Levesque, Ms. R. Herrington and Ms. P. Salami for helping with the recording procedures and data analysis. We also thank Dr. Kai Kaila for generously providing us with benzolamide.

References

Alger BE, Nicoll RA. Pharmacological evidence for two kinds of GABA receptor on rat hippocampal pyramidal cells studied in vitro. J Physiol. 1982; 328:125–141. [PubMed: 7131310]

Andersen P, Dingledine R, Gjerstad L, Langmoen IA, Laursen AM. Two different responses of hippocampal pyramidal cells to application of gamma aminobutyric acid. J Physiol. 1980; 305:279–296. [PubMed: 7441554]

Autere AM, Lamsa K, Kaila K, Taira T. Synaptic activation of $GABA_A$ receptors induces neuronal uptake of Ca^{2+} in adult hippocampal slices. J Neurophysiol. 1999; 81:811–815. [PubMed: 10036281]

Avoli M. Epileptiform discharges and a synchronous GABAergic potential induced by 4-aminopyridine in the rat immature hippocampus. Neurosci Lett. 1990; 117:93–98. [PubMed: 1963215]

Avoli M, de Curtis M. GABAergic synchronization in the limbic system and its role in the generation of epileptiform activity. Prog Neurobiol. 2011; 95:104–132. [PubMed: 21802488]

Avoli M, Panuccio G, Herrington R, D'Antuono M, de Guzman P, Lévesque M. Two different interictal spike patterns anticipate ictal activity in vitro. Neurobiol Dis. 2013; 52:168–176. [PubMed: 23270790]

Bénar CG, Chauviére L, Bartolomei F, Wendling F. Pitfalls of high-pass filtering for detecting epileptic oscillations: a technical note on "false" ripples. Clin Neurophysiol. 2010; 121:301–310. [PubMed: 19955019]

Blaesse P, Airaksinen MS, Rivera C, Kaila K. Cation-chloride cotransporters and neuronal function. Neuron. 2009; 61:820–838. [PubMed: 19323993]

Bragin A, Benassi SK, Kheiri F, Engel J. Further evidence that pathological high frequency oscillations are bursts of population spikes derived from recordings of identified cells in dentate gyrus. Epilepsia. 2011; 52:45–52.

Buzsaki G, Horvath Z, Urioste R, Hetke J, Wise K. High-frequency network oscillation in the hippocampus. Science. 1992; 256:1025–1027. [PubMed: 1589772]

Dodgson SJ, Shank RP, Maryanoff BE. Topiramate as an inhibitor of carbonic anhydrase isoenzymes. Epilepsia. 2000; 41:S35–S39.

Dzhala VI, Staley KJ. Transition from interictal to ictal activity in limbic networks in vitro. J Neurosci. 2003; 23:7873–7880. [PubMed: 12944517]

Engel J Jr, Bragin A, Staba R, Mody I. High-frequency oscillations: what is normal and what is not? Epilepsia. 2009; 50:598–604. [PubMed: 19055491]

Farrant M, Kaila K. The cellular, molecular and ionic basis of GABA(A) receptor signaling. Prog Brain Res. 2007; 160:59–87. [PubMed: 17499109]

Grover LM, Lambert NA, Schwartzkroin PA, Teyler TJ. Role of HCO3- ions in depolarizing $GABA_A$ receptor-mediated responses in pyramidal cells of rat hippocampus. J Neurophysiol. 1993; 69:1541–1555. [PubMed: 8389828]

Hamidi S, Lévesque M, Avoli M. Epileptiform synchronization and highfrequency oscillations in brain slices comprising piriform and entorhinal cortices. Neuroscience. 2014; 281:258–268. [PubMed: 25290016]

Herrington R, Lévesque M, Avoli M. Neurosteroids modulate epileptiform activity and associated high-frequency oscillations in the piriform cortex. Neuroscience. 2014; 256:467–477. [PubMed: 24157930]

Hübner CA, Holthoff K. Anion transport and GABA signaling. Front Cell Neurosci. 2013; 7:177. [PubMed: 24187533]

Jefferys, JGR., Jiruska, P., de Curtis, M., Avoli, M. Limbic network synchronization and temporal lobe epilepsy. In: Noebels, JL.Avoli, M.Rogawski, MA.Olsen, RW., Delgado-Escueta, AV., editors. Jasper's Basic Mechanisms of the Epilepsies. National Center for Biotechnology Information (US); Bethesda (MD): 2012a.

Jefferys JGR, Menendez de la Prida L, Wendling F, Bragin A, Avoli M, Timofeev I, Lopes da Silva FH. Mechanisms of physiological and epileptic HFO generation. Prog Neurobiol. 2012b; 98:250–264. [PubMed: 22420980]

Johnston D, Brown TH. Giant synaptic potential hypothesis for epileptiform activity. Science. 1981; 16:294–297.

Kaila K. Ionic basis of $GABA_A$ receptor channel function in the nervous system. Prog Neurobiol. 1994; 42:489–537. [PubMed: 7522334]

Kaila K, Lamsa K, Smirnov S, Taira T, Voipio J. Long-lasting GABA-mediated depolarization evoked by high-frequency stimulation in pyramidal neurons of rat hippocampal slice is attributable to a network-driven, bicarbonate-dependent K^+ transient. J Neurosci. 1997; 17:7662–7672. [PubMed: 9315888]

Krnjević K. Chemical nature of synaptic transmission in vertebrates. Physiol Rev. 1974; 54:418–540.

Lévesque M, Salami P, Gotman J, Avoli M. Two seizure-onset types reveal specific patterns of high-frequency oscillations in a model of temporal lobe epilepsy. J Neurosci. 2012; 32:13264–13272. [PubMed: 22993442]

Lillis KP, Kramer MA, Mertz J, Staley KJ, White JA. Pyramidal cells accumulate chloride at seizure onset. Neurobiol Dis. 2012; 47:358–366. [PubMed: 22677032]

Miles, R., Blaesse, P., Huberfeld, G., Wittner, L., Kaila, K. Chloride homeostasis and GABA signaling in temporal lobe epilepsy. In: Noebels, JL.Avoli, M.Rogawski, MA.Olsen, RW., Delgado-Escueta, AV., editors. Jasper's Basic Mechanisms of the Epilepsies. National Center for Biotechnology Information (US); Bethesda (MD): 2012.

Payne JA, Rivera C, Voipio J, Kaila K. Cation-chloride co-transporters in neuronal communication, development and trauma. TrendsNeurosci. 2003; 4:199–206.

Perez Velazquez JL. Bicarbonate-dependent depolarizing potentials in pyramidal cells and interneurons during epileptiform activity. Eur J Neurosci. 2003; 18:1337–1342. [PubMed: 12956733]

Rivera C, Voipio J, Kaila K. Two developmental switches in GABAergic signalling: the K^+-Cl^- cotransporter KCC2 and carbonic anhydrase CAVII. J Physiol. 2005; 562:27–36. [PubMed: 15528236]

Ruusuvuori E, Li H, Huttu K, Palva JM, Smirnov S, Rivera C, Kaila K, Voipio J. Carbonic anhydrase isoform VII acts as a molecular switch in the development of synchronous gamma-frequency firing of hippocampal CA1 pyramidal cells. J Neurosci. 2004; 24:2699–2707. [PubMed: 15028762]

Ruusuvuori E, Huebner AK, Kirilkin I, Yukin AY, Blaesse P, Helmy M, Kang HJ, El Muayed M, Hennings JC, Voipio J, Šestan N, Hübner CA, Kaila K. Neuronal carbonic anhydrase VII provides GABAergic excitatory drive to exacerbate febrile seizures. EMBO J. 2013; 32:2275–2286. [PubMed: 23881097]

Salami P, Lévesque M, Gotman J, Avoli M. A comparison between automated detection methods of high-frequency oscillations (80–500 Hz) during seizures. J Neurosci Methods. 2012; 211:265–271. [PubMed: 22983173]

Schwartzkroin PA, Prince DA. Cellular and field potential properties of epileptogenic hippocampal slices. Brain Res. 1978; 147:117–130. [PubMed: 656907]

Schwartzkroin PA, Prince DA. Changes in excitatory and inhibitory synaptic potentials leading to epileptogenic activity. Brain Res. 1980; 183:61–73. [PubMed: 6244050]

Schwiening CJ, Boron WF. Regulation of intracellular pH in pyramidal neurones from the rat hippocampus by Na(+)-dependent Cl(−)-HCO3- exchange. J Physiol. 1994; 475:59–67. [PubMed: 8189393]

Staley, KJ. Role of the depolarizing GABA response in epilepsy. In: Binder, Devin K., Scharfman, Helen E., editors. Recent Advances in Epilepsy Research. Kluwer Academic/Plenum Publishers; USA: 2004.

Staley KJ, Soldo BL, Proctor WR. Ionic mechanisms of neuronal excitation by inhibitory $GABA_A$ receptors. Science. 1995; 269:977–981. [PubMed: 7638623]

Stinger JL. A comparison of topiramate and acetazolamide on seizure duration and paired-pulse inhibition in the dentate gyrus of the rat. Epilepsy Res. 2000; 40:147–153. [PubMed: 10863142]

Supuran CT, Scozzafava A, Casini A. Carbonic anhydrase inhibitors. Med Res Rev. 2003; 23:146–189. [PubMed: 12500287]

Traub RD, Borck C, Colling SB, Jefferys JG. On the structure of ictal events in vitro. Epilepsia. 1996; 37:879–891. [PubMed: 8814102]

Viitanen T, Ruusuvuori E, Kaila K, Voipio J. The K^+-Cl^- cotransporter KCC2 promotes GABAergic excitation in the mature rat hippocampus. J Physiol. 2010; 588:1527–1540. [PubMed: 20211979]

Voipio J, Kaila K. GABAergic excitation and K (+)-mediated volume transmission in the hippocampus. Prog Brain Res. 2000; 125:329–338. [PubMed: 11098669]

Ylinen A, Bragin A, Nádasdy Z, Jandó G, Szabó I, Sik A, Buzsáki G. Sharp wave-associated high-frequency oscillation (200 Hz) in the intact hippocampus: network and intracellular mechanisms. J Neurosci. 1995; 15:30–46. [PubMed: 7823136]

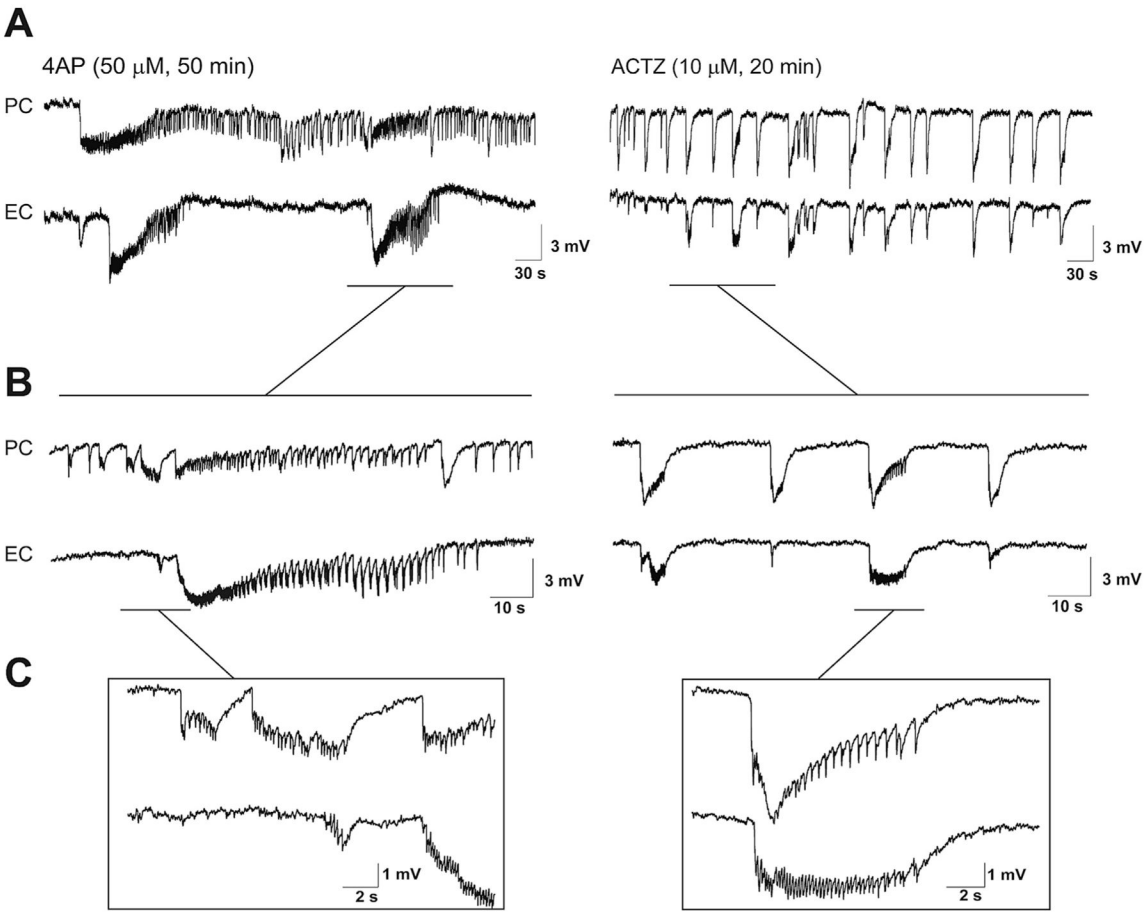

Fig. 1.

A: Field potential recordings obtained from PC and EC under control (4AP, 50 μM, 50 min) conditions and during 20 min application of 10 μM ACTZ (n = 10 experiments). **B** and **C**: Enlarged portions of the recordings traces shown in **A**. Note that the pattern of interictal–ictal epileptiform discharge is disrupted after application of ACTZ (10 μM), and in particular long-lasting ictal events associated to distinct tonic-clonic electrographic activity are abolished in both PC and EC.

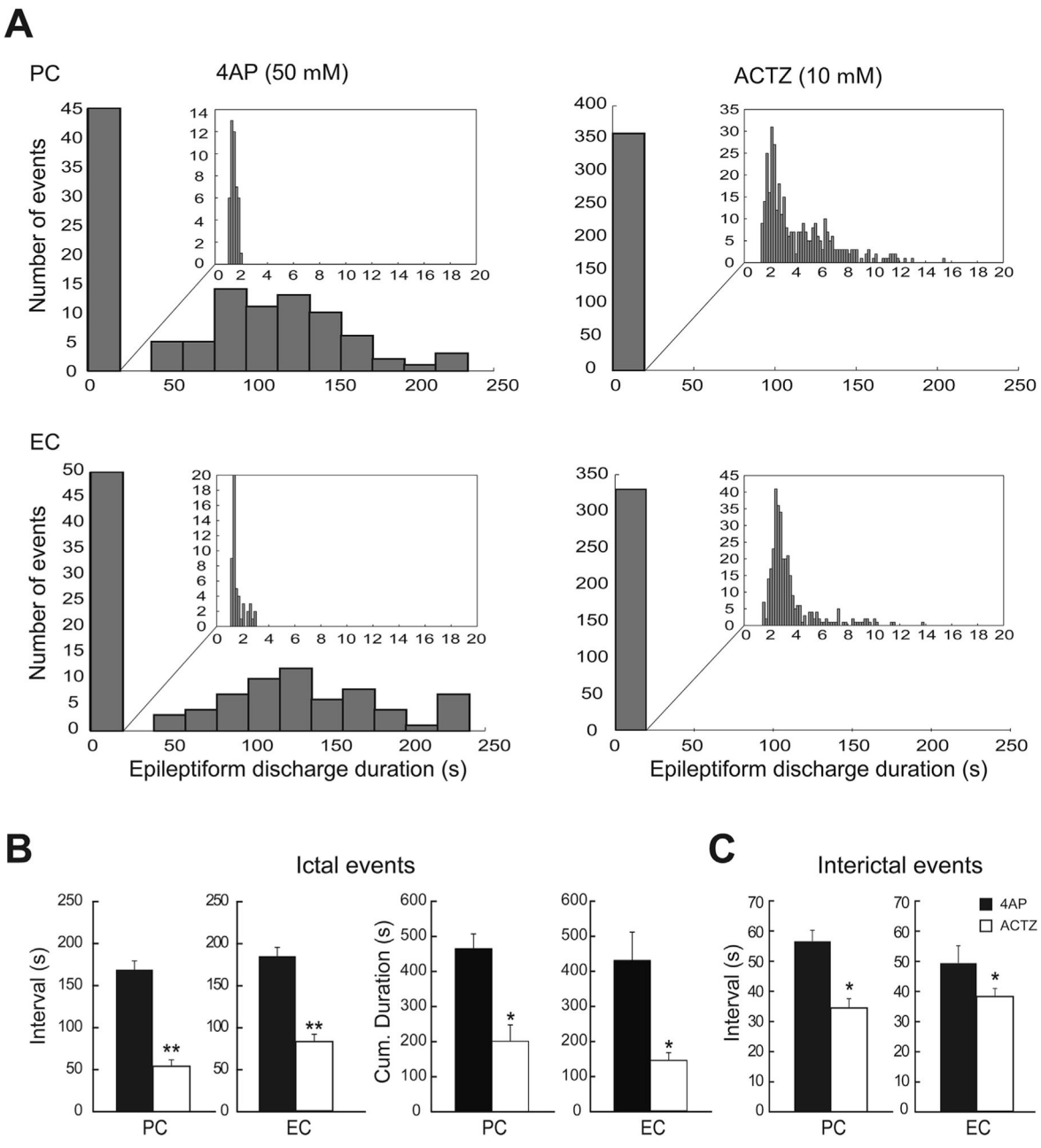

Fig. 2.

A: Distribution histograms of the duration of the epileptiform discharges recorded from PC and EC during control (4AP, 50 μM) and during application of 10 μMACTZ (n = 10 experiments). Note that ACTZ (10 μM) modulated the duration of epileptiform discharges in both regions, causing a significant change in the distribution of epileptiform discharges duration and specifically disappearance of prolonged ictal events. **B**: Bar graphs showing the average interval of occurrence and cumulative duration of ictal discharges recorded from the PC and EC in control and during ACTZ (10 μM) application. **C**: Bar graphs showing the average interval of occurrence of interictal discharges recorded from PC and EC during

control 4AP (50 μM) and application of ACTZ (10 μM). Note that the interval of occurrence of both ictal and interictal discharges are significantly reduced after application of ACTZ (10 μM) in both regions. ACTZ (10 μM) also reduced the cumulative duration of ictal discharges in both regions. *$p < 0.01$, **$p < 0.0001$.

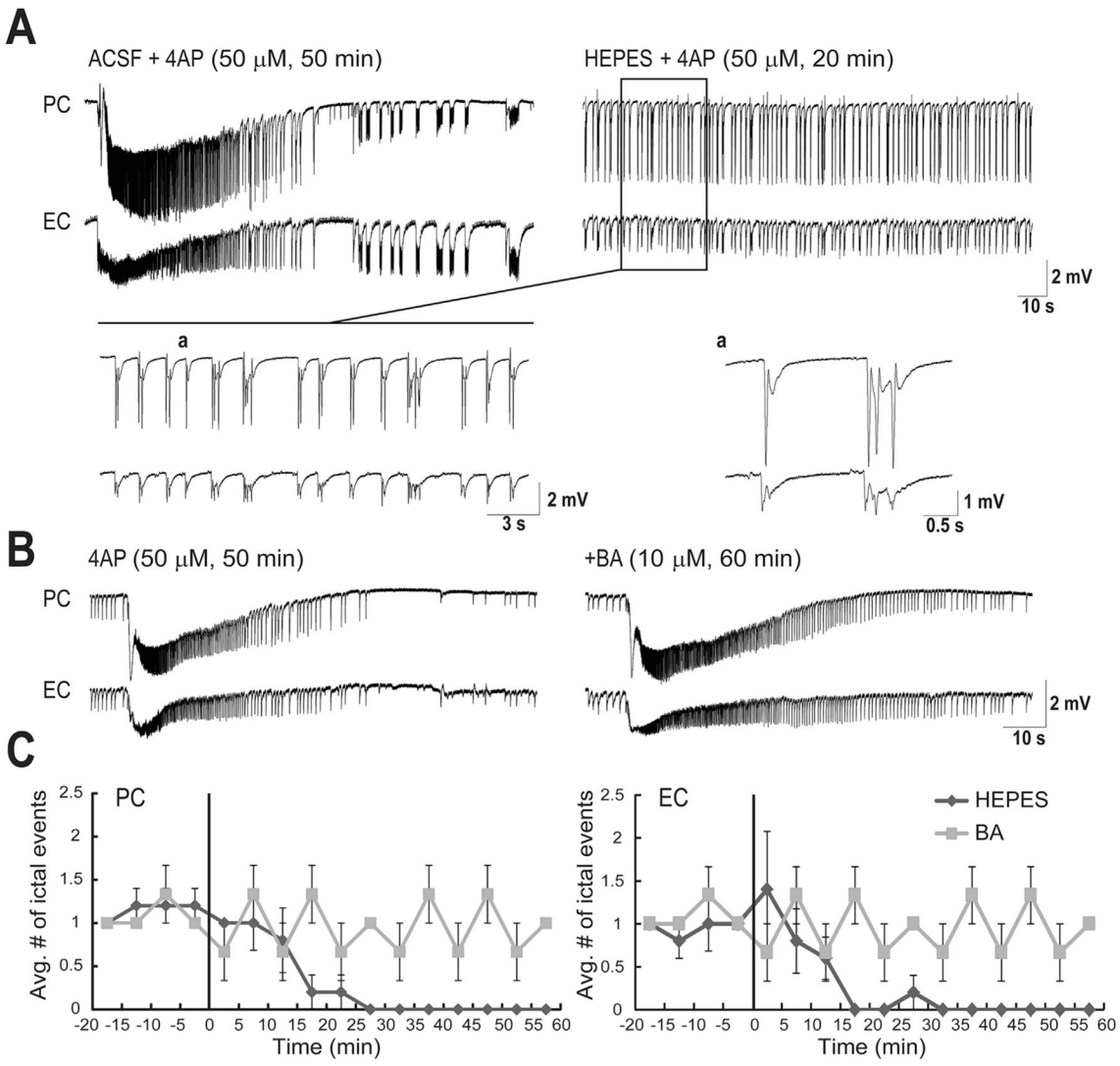

Fig. 3.

A: Field potential recordings obtained from PC and EC regions during 50 min application of 4AP (10 μM) and HCO_3^--free HEPES-buffered solution (20 min, n = 6 experiments). Note that HCO_3^--free HEPES-buffered solution virtually abolishes ictal discharges in both brain regions whereas interictal discharges continue to occur. Enlarged portion of the recordings during HCO_3^--free HEPES-buffered solution are shown in insets with traces that are further expanded during interictal activity. **B**: Field potential recordings obtained from PC and EC areas during 50 min application of 4AP (50 μM) and 60 min BA (10 μM, n = 4 experiments). **C**: Plots showing the average number of ictal discharges in PC and EC. Vertical lines in both graphs indicate the application of BA or HCO_3^--free HEPES-buffered solution. Note that after 20 min bath application of HCO_3^--free HEPES-buffered solution the occurrence of ictal discharges in both PC and EC were blocked while ictal discharges continued to occur at the same frequency after application of BA (10 μM).

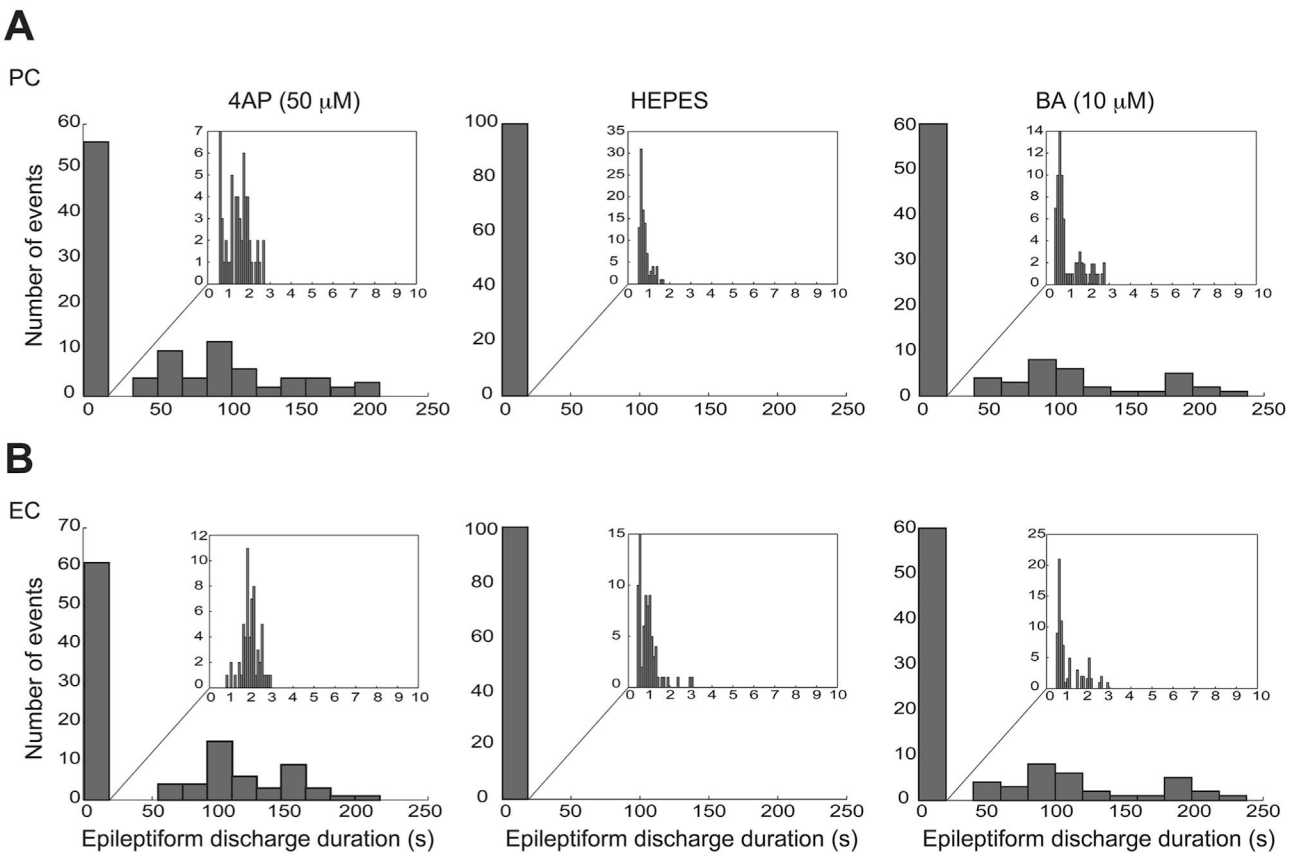

Fig. 4.

A and **B**: Distribution histograms of the duration of the epileptiform discharges recorded from PC (**A**) and EC (**B**) during control (4AP, 50 μM) and during application of either HCO_3^--free HEPES-buffered solution (n = 6 experiments) or BA (10 μM, n = 4 experiments). Note that HCO_3^--free HEPES-buffered solution modulated the duration of epileptiform discharges in both regions, causing a significant change in the distribution of epileptiform discharges duration and specifically disappearance of prolonged ictal events whereas BA (10 μM) did not affect the distribution of epileptiform discharges duration.

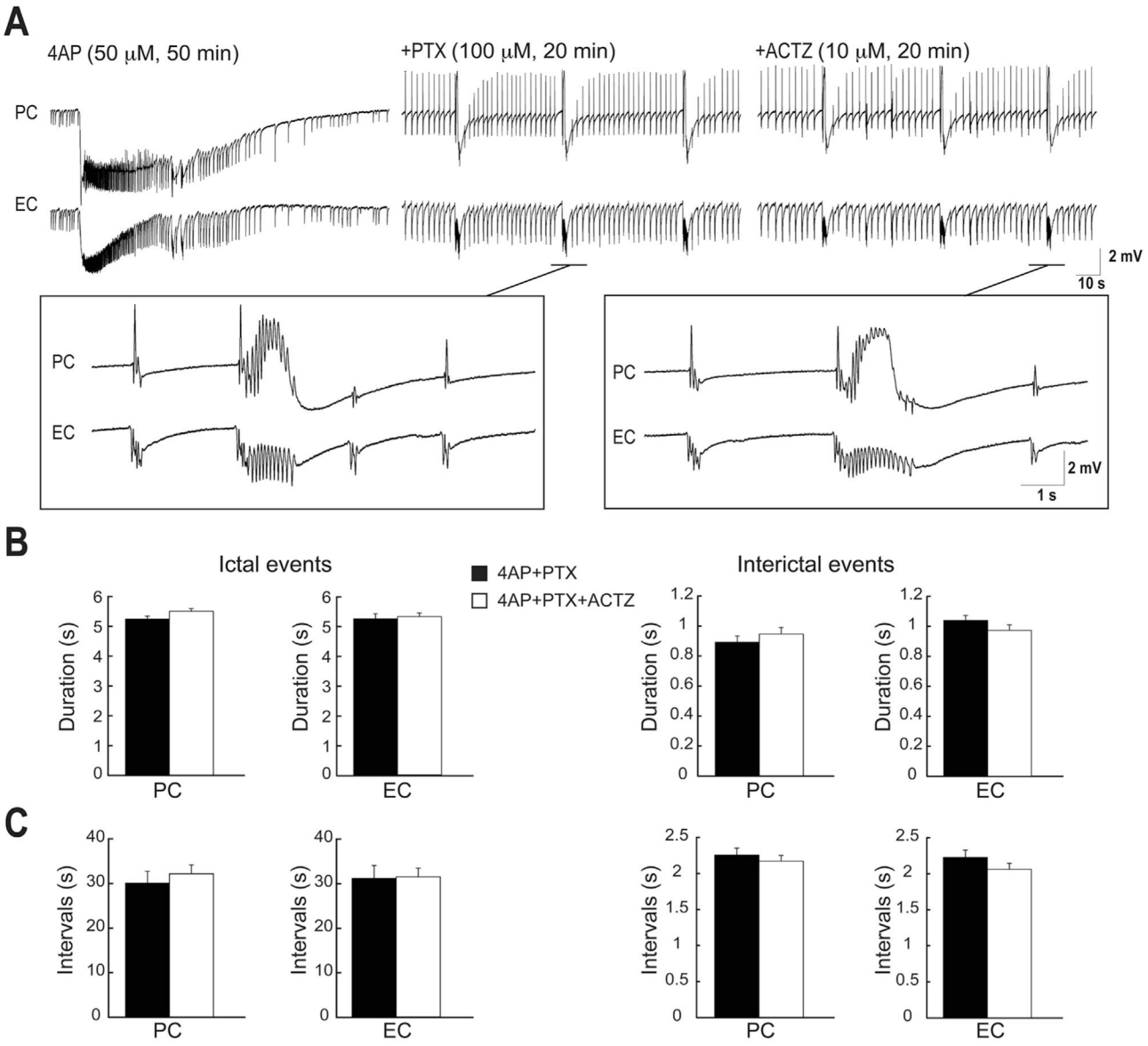

Fig. 5.

A: Field potential recordings obtained from PC and EC areas during application of 4AP (50 μM), PTX (100 μM) and ACTZ (10 μM, n = 6 experiments). Note that PTX abolishes long-lasting ictal discharges in both brain regions whereas interictal discharges continue to occur. Enlarged portion of the recordings during 4AP + PTX and 4AP + PTX + ACTZ are shown in insets. **B**: Bar graphs showing the average duration of ictal and interictal discharges recorded from the PC and EC in 4AP + PTX and during 4AP + PTX + ACTZ application. **C**: Bar graphs showing the average interval of occurrence of ictal and interictal discharges recorded from PC and EC during 4AP + PTX and 4AP + PTX + ACTZ. Note that further application of ACTZ (10 μM) does not affect neither the duration and nor the interval of epileptiform events.

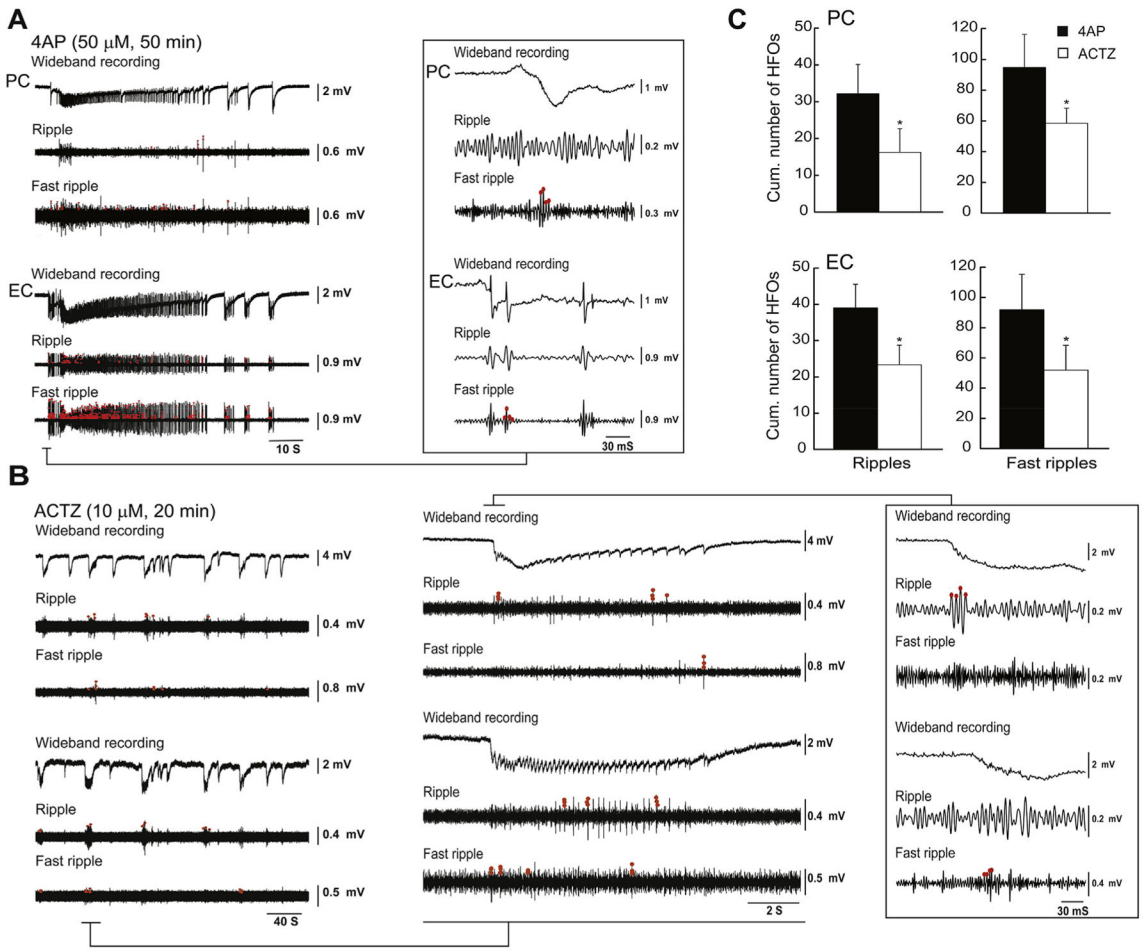

Fig. 6.

A: Under control conditions both ripples and fast ripples occur during an ictal discharge recorded from the PC and EC under control (4AP, 50 μM) conditions (n = 10 experiments). Ripples and fast ripples are indicated by the red dots. **B**: Both types of HFOs decrease in rate during application of ACTZ (10 μM) as also shown in the enlarged portion of the recordings in the inset. **C**: Bar graphs showing the cumulative number of ripples and fast ripples associated with ictal discharges during control 4AP (50 μM) and application of ACTZ (10 μM) in PC and EC. *$p < 0.05$. (For interpretation of the references to color in this figure legend, the reader is referred to the web version of this article.)

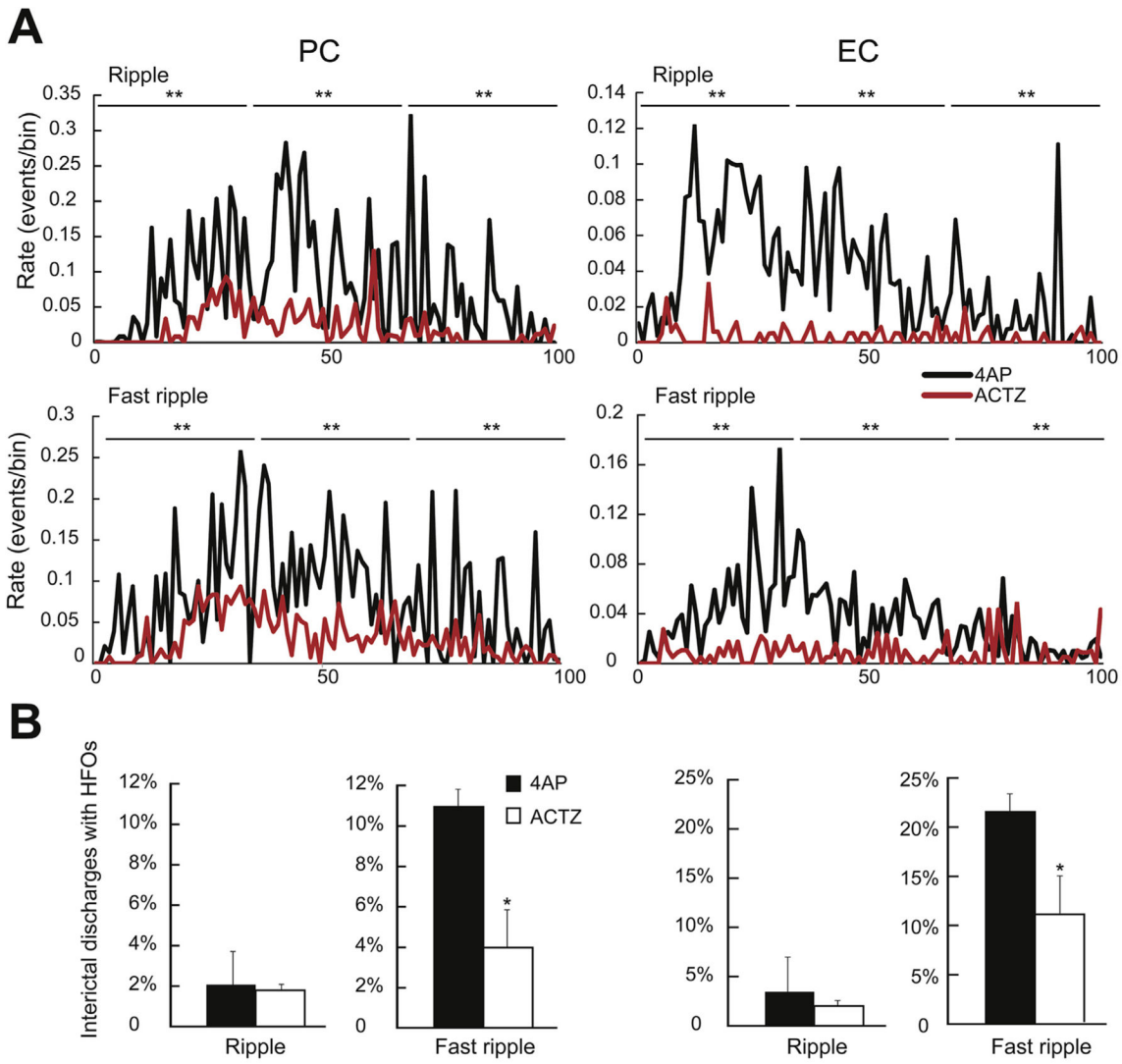

Fig. 7.

A: Rate of occurrence of ripples and fast ripples during ictal discharges recorded from the PC and the EC during control (4AP, 10 μM) and during application of ACTZ (10 μM, n = 10 experiments). The duration of the ictal discharges was normalized from 0 (start of the ictal discharge) to 100 (end of the ictal discharge) to account for different durations. Note that in both PC and EC, the rates of occurrence of ripples and fast ripples throughout the ictal discharges are reduced by ACTZ (10 μM). **B**: Bar graphs showing the proportion of interictal discharge co-occurring with ripples and fast ripples in PC and EC under control conditions and in the presence of ACTZ (10 μM). Note that in both regions the percentage of interictal discharges co-occurring with fast ripples is reduced by ACTZ (10 μM). *$p < 0.05$, **$p < 0.001$.

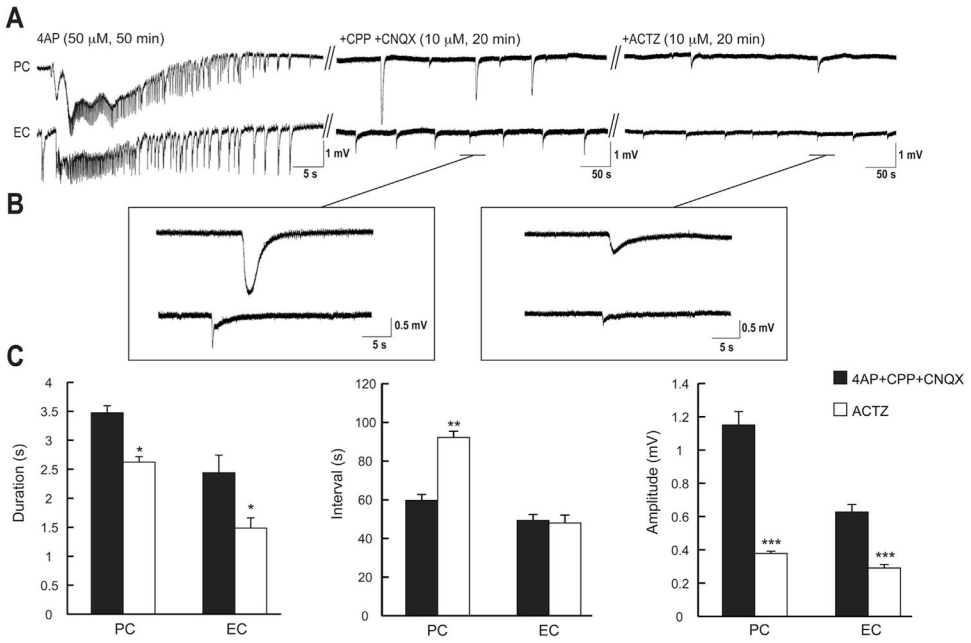

Fig. 8.

A: Effects induced by 20 min application of ACTZ (10 μM) on the isolated GABAergic field events occurring in the PC and EC during 20 min concomitant application of CPP + CNQX (10 μM each, n = 6 experiments). In panel **A** the initial control activity under 4AP treatment is characterized by a typical tonic-clonic ictal discharges in both PC and EC. Enlarged portion of these events shown in **B** during application of CPP + CNQX (10 μM each) and after application of ACTZ (10 μM). **C**: Bar graphs summarizing the change in duration, interval of occurrence and amplitude of the slow isolated GABAergic events under control conditions (i.e., 4AP + CPP + CNQX) and during further application of ACTZ (10 μM). Note that application of ACTZ (10 μM) decreases the duration, the rate of occurrence and the amplitude of these events. *$p < 0.05$, **$p < 0.001$, ***$p < 0.0001$.